Electronic Supplementary Information

Synergistic Ternary Polypyrrole/WO_3/MWCNT Nanocomposites for Environmental Remediation and Electrochemical Water Splitting

Nafees Ahmad[†a], Greesh Kumar[†b], Irfanul Haq Faridi[c], Ramendra Sundar Dey*[b]

[a] *Department of Chemistry, Integral University, Lucknow, Uttar Pradesh, 226026, India*

[b] *Institute of Nano Science and Technology (INST), Sector-81, Mohali-140306, Punjab, India*

[c] *Interdisciplinary Biotechnology Unit, Aligarh Muslim University, Aligarh, 202002, India*

[†] *These authors contributed equally to this work.*

Corresponding Author: rsdey@inst.ac.in

1. Material Characterizations

The synthesized materials were characterized by X-ray diffraction technique (XRD- BRUKER D8 ADVANCE 30 kV and 15 mA) to study the crystal size and geometry and the analysis of functional groups was performed by FTIR (Fourier transform infrared spectroscopy- Perkin Elmer spectrum-2, USA) in range of 400-4000 cm-1. Surface morphology and elemental composition were studied by SEM-EDX (JSM 6510 LV JEOL Japan). Ultraviolet-visible spectroscopy (Thermo scientific Evolution 201- USA) was used to check the absorbance of PBS samples and the recombination behavior of photo-induced charge carriers was examined by photoluminescence intensity through fluorescence spectroscopy (Hitachi- F-2500- Japan) at an excitation wavelength of 562 nm. The surface area, pore size, and pore volumes were calculated by Brunauer–Emmett–Teller (Quantachrome Instruments version 5.21). X-ray photoelectron spectroscopy (XPS) analysis was performed XPS spectrometer (K-Alpha 1063) instruments in an ultrahigh vacuum chamber (7X10-9 torr) using Al-Kα radiation (1486.6 eV).

2. Calculations

2.1. Adsorption activity

A dynamic method was used to study the adsorption property of PPy/WO_3/MWCNT against PBS dye in which 100 mg of PPy/WO_3/MWCNT was dispersed in the PBS solution under continuous stirring. One the adsorption equilibrium has achieved, the mixture aqueous solution of PBS and

PPy/WO_3/MWCNT were taken out of the reactor at regular interval to check the absorbance at maximum absorption wavelength λmax = 510 nm. The amount of PBS adsorbed by PPy/WO_3/MWCNT was calculated by the following equation (1).

$$\text{Amount of PBS adsorbed} = \frac{C0 - Ce}{M} * V \qquad \text{Eq. (1)}$$

In the above equation, C_0 and Ce are the initial and the equilibrium concentration of the PBS and V (L) and M (g) are the volume of PBS solution and mass of the PPy/WO_3/MWCNT respectively. The obtained data were used to study the adsorption thermodynamics using Langmuir and Freundlich adsorption isotherm and adsorption kinetics using pseudo-first-order (adsorption) and pseudo-second-order (diffusion). In addition, the adsorption efficiency (% AE) of PPy/WO_3/MWCNT against PBS was calculated by following equation (2)

$$\text{Adsorption efficiency (\%)} = \frac{C0 - Ct}{C0} * 100\% \qquad \text{Eq. (2)}$$

2.2. Photocatalytic, Scavenging and durability test

The photocatalytic studies of PPy/WO_3/MWCNT were performed in the photochemical rector equipped with visible lamp and oxygen pump water circulation tank to maintain the temperature. Before the photodegradation process, adsorption study has been carried out in which the PBS and PPy/WO_3/MWCNT were mixed and kept for stirring without illumination for 1 hr. The samples were taken out at a regular interval to check the adsorption of PBS on the surface of PPy/WO_3/MWCNT. Once the adsorption−diffusion equilibrium achieved between the PBS and PPy/WO_3/MWCNT, a visible lamp (power 500 W) was illuminated to the mixture kept on continuous stirring. Further, 5 mL of PBS sample were taken out of the reactor at regular interval of time, centrifuged and then absorbance was measured at maximum absorption wavelength of λ_{max} = 510 nm for PBS dye. The obtained data were used to study the kinetics and rate constant calculation of photocatalysts. The amount of PBS degraded by PPy/WO_3/MWCNT was calculated by using the following equation (3)

Amount of dye adsorbed $= \frac{C_e - C_t}{M} * V$ Eq. (3)

In equation 3, C_e and C_t are the concentration of PBS dye at adsorption equilibrium and at a time't' respectively, V (L) and M (g) are the volume of dye solution, and mass of the photocatalysts respectively. Further, the degradation efficiency (%) of the PPy/WO_3/MWCNT against the PBS was calculated by following equation (4).

Degradation efficiency (%) $= \frac{C_e - C_t}{C_e} \times 100\%$ Eq. (4)

Another experiment was also performed to confirm the formation of ROS and their accountability for the photodegradation. For this experiment, four different scavengers isopropyl alcohol (IPA), p-benzoquinone, and sodium ethylenediaminetetraacetic acid (Na-EDTA) and sodium nitrate ($NaNO_3$) was used to quench •OH, $\bullet O_2^-$, h^+ and e^- respectively. To perform this experiment, 2mM each scavengers were added during the photocatalytic degradation of PBS dye. In addition, durability test was also performed to check the stability of PPy/WO_3/MWCNT in which the photocatalyst was recovered after the experiment, washed with acetone, dried ate 60^0C and again used for the photocatalytic experiment for the six cycles. The results of the photocatalytic activity shows the stability of the catalyst against the PBS dye.

2.3. Electrochemical study

CHI 760E electrochemical workstation, and BioLogic VSP potentiostats electrochemical workstation were used to check the electrochemical activity of catalysts by using three electrode setup. For the experimental set up, catalyst material loaded nickel foam (1*1 cm^2 area) were used as the working electrode along with graphite rode (3mm diameter) as counter electrode. The Hg/$HgSO_4$ electrode used for OER-HER study in alkaline media. The electrochemical activity of PPy/WO_3/MWCNT and other catalysts were measured using electrochemical workstation by employing (CV), (LSV), and Chronoamperometry Technique (CA) techniques using 1.0 M KOH as electrolyte solution at room temperature. Our synthesized material was drop casted on a pre-

cleaned nickel foam electrodes and it can be used as the working electrode. To prepare the catalytic ink, 10 mg of the synthesized catalyst was dispersed in 1 mL of a 1:1 (v/v) isopropanol and deionized (DI) water mixture containing 5 wt% Nafion solution, followed by sonication for 1 hour to obtain a homogeneous suspension. For comparison, Pt/C (20 wt%) and RuO_2 catalyst inks were prepared similarly by dispersing 10 mg of the respective catalysts in the same solvent mixture with Nafion (5 wt%) and ultrasonicated for 1 hour. The resulting inks were drop-casted onto pre-cleaned nickel foam substrates to achieve a catalyst loading of 0.9 mg cm^{-2}, which served as the working electrode for all electrochemical measurements. For two-electrode water-splitting experiments, a mixed catalyst ink containing Pt/C and RuO_2 in a 1:1 mass ratio (10 mg total) was prepared under identical conditions and drop-casted onto the nickel foam at the same loading (0.9 mg cm^{-2}). Mott-Schottky (M-S) analysis was carried out in 1.0 M KOH alkaline solution at 10 Hz frequency.

The calculation of Tafel slope for OER and HER

The potential coverted to RHE using equation below:

$$\boldsymbol{E_{RHE} = (E_{Hg/HgSO4\ (saturated)} + 0.65 + 0.0591\ pH)\ V} \quad \text{Eq. (5)}$$

$$\boldsymbol{\eta = a + b * \log j} \quad \text{Eq. (6)}$$

where $\boldsymbol{\eta}$ is known as the overpotential, j is represented as the current density, and b is the Tafel slope. All the onset potentials were calculated based on the very beginning of the linear region in Tafel plots.

The calculation of overpotential for OER

$$\boldsymbol{\eta = E_{RHE} - 1.23} \quad \text{Eq. (7)}$$

The electrochemical active surface area analysis of PPy/WO_3/MWCNT, WO_3 and PPy catalysts have been done by using cyclic voltammetry curve which were taken with three electrode system at different scan rates from 10 to 80 mV s^{-1} in 1.0 M KOH electrolyte solution on modifying the materials on glassy carbon (3 mm diameter) electrode. The CV curves in a non-faradaic region were plotted as a function of various scan rates (10, 20, 40, 60, and 80 mV s^{-1}). Double layer capacitance (C_{dl}) for as prepared PPy/WO_3/MWCNT, WO_3 and PPy catalyst materials calculated from the slope of the linear regression between the current density differences in the middle of the potential window of CV curves vs the scan rates. The C_s is the specific capacitance of the electrode

and was taken as 40 μFcm^{-2}. The electrochemical surface area (ECSA) was calculated by using following equation which is give below.

$$ECSA = \frac{C_{dl}}{C_s} \quad \text{Eq. (8)}$$

Faradaic efficiency calculation

Faradaic efficiency of water splitting catalyzed by using PPy/WO_3/MWCNT composite material was calculated by dividing the amount of the experimentally evolved gas by the theoretical amount of gas which is calculated by the charge passed through the electrode:

Faradaic efficiency (FE) of H_2 = $V_{experimental}$ / $V_{theoretical}$ = $V_{experimental}$ / [(2/4)*(Q/F)*Vm]

Eq. (9)

Faradaic efficiency (FE) of O_2 = $V_{experimental}$ / $V_{theoretical}$ = $V_{experimental}$ / [(1/4)*(Q/F)*Vm]

Eq. (10)

Where Q is the summation of the charge passed through the anode and cathode electrodes, F is the Faraday constant (96485 C mol^{-2}), the number 2 means 2 moles of H_2 per mole of H_2O, the number 4 means 4 moles of electrons per mole of H_2O, the number 1 means 1 mole of O_2 per mole of H_2O and Vm is the molar volume of gas (24.1 L mol^{-1}, 293 K, 101 kPa).

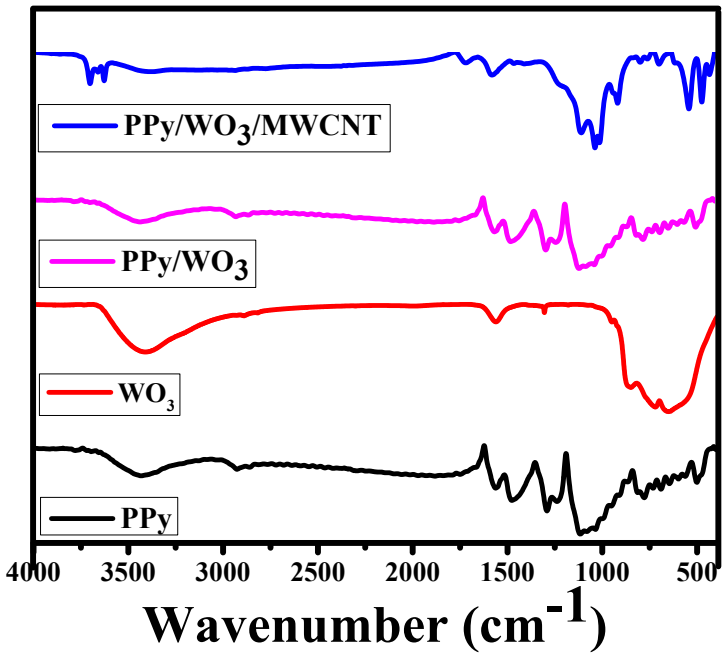

Fig. S1. FTIR spectra of the synthesized photocatalysts

Fig. S2. Particle size distribution of PPy/WO_3/MWCNT material

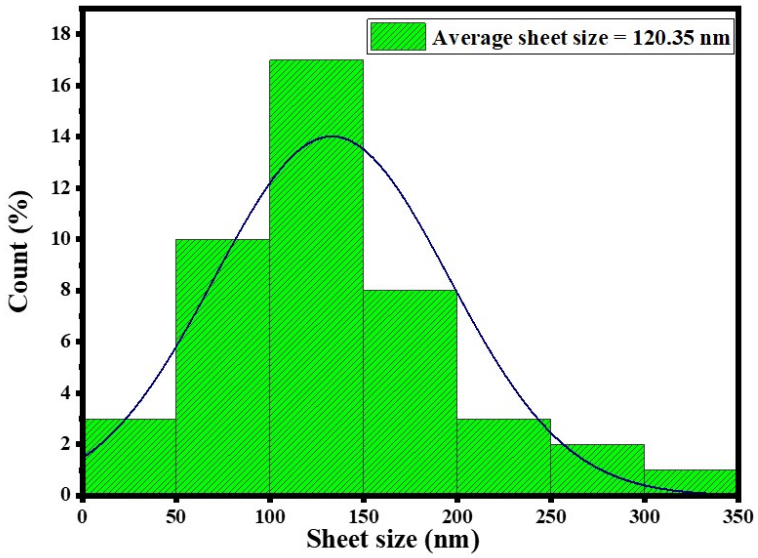

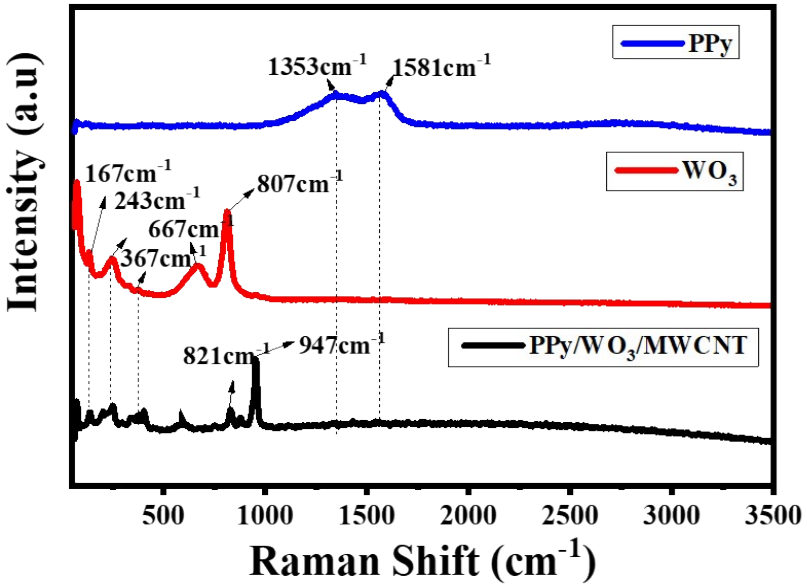

Fig. S3. Raman spectra of the PPy/WO_3/MWCNT nanocomposite, PPy and WO_3 materials.

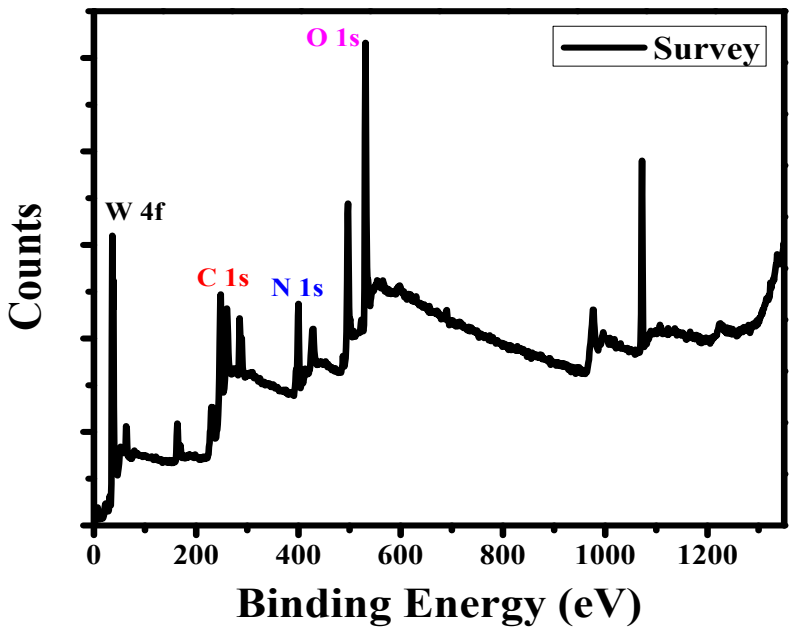

Fig. S4. XPS survey of $PPy/WO_3/MWCNT$

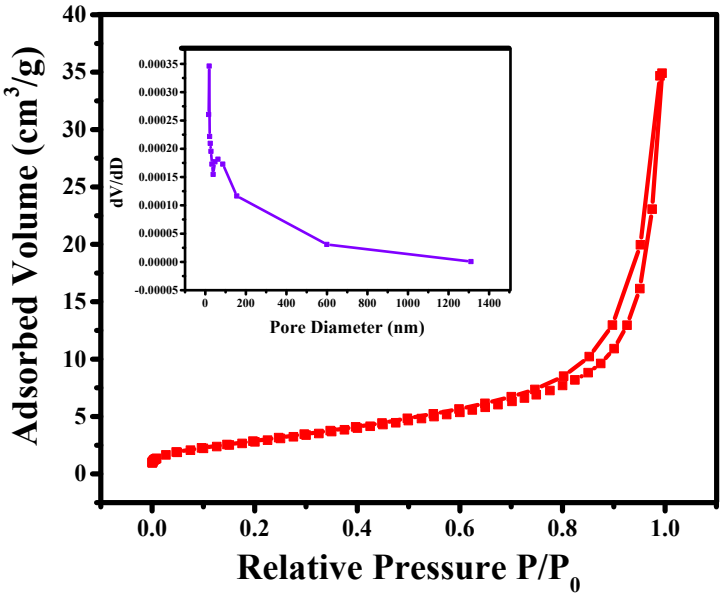

Fig. S5. BET isotherm of PPy/WO_3 photocatalyst

2.4. Band gap Analysis

The band gap of the prepared nanoparticle as well as polymer matrix were calculated by using Kubelka Munk Function using the formula (11) and (12)

$$(h\nu.\alpha) = (Ah\nu\text{-}Eg)^{n/2} \qquad \text{Eq. (11)}$$

Where α is the proportionality constant kubelka Munk Function F(R), then the expression becomes

$$(h\nu.F(R)) = (Ah\nu\text{-}Eg)^{n/2} \qquad \text{Eq. (12)}$$

Where ν is the frequency of light, F(R) is the Kubelka Munk Function; A is the proportionality constant and Eg is the bandgap energy. The value of n can be determined by the type of optical transition n=1 for direct and n=4 for indirect transition.

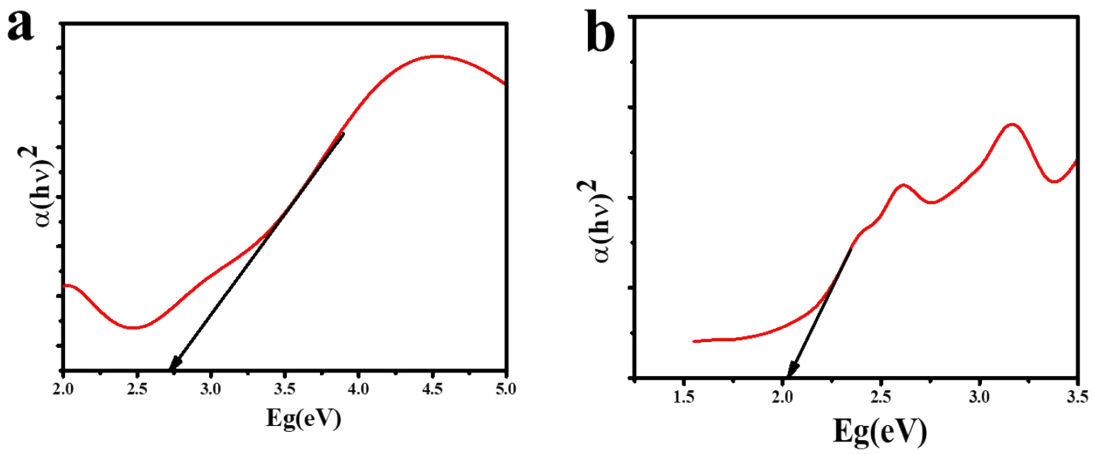

Fig. S6 (a) Tauc plot of WO_3 and (b) PPy/WO_3

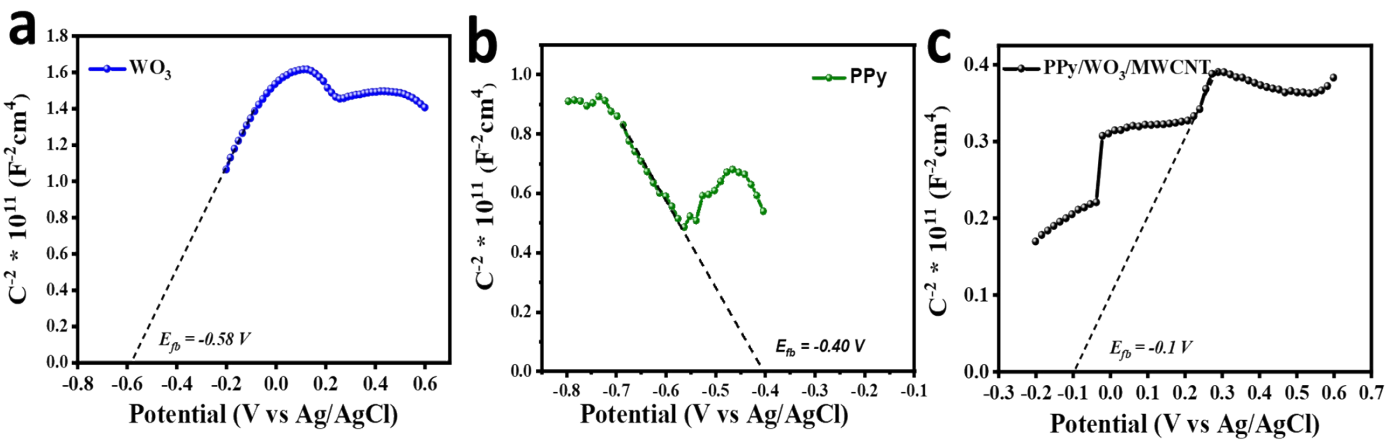

Fig. S7. Mott-Schottky plots of (a) WO_3, (b) PPy and (c) PPy/WO_3/MWCNT catalyst materials

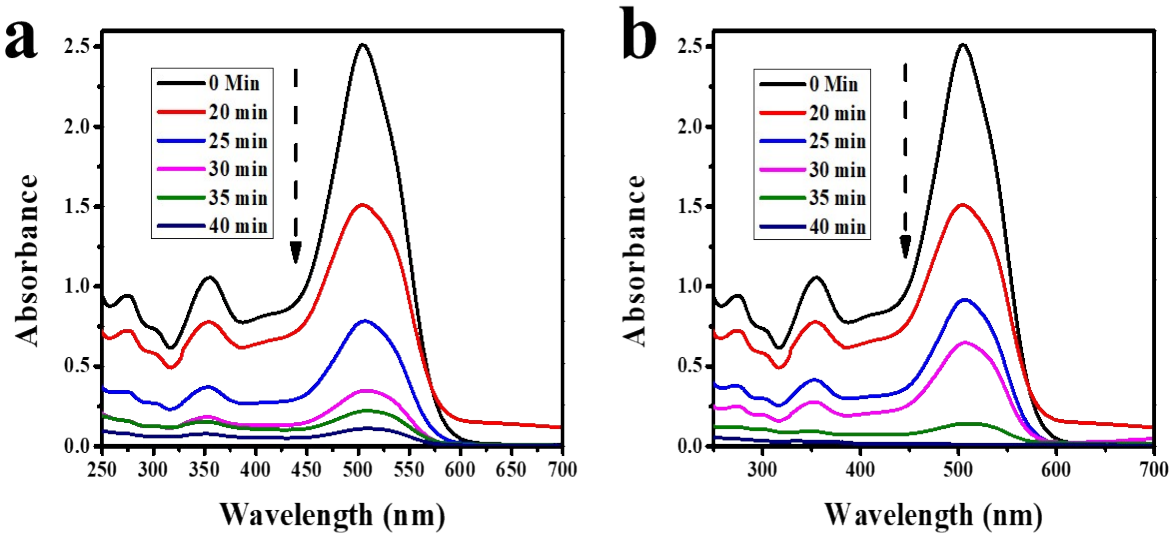

Fig. S8 (a) UV-visible spectra of the degraded samples of PBS dye by PPy (b) PPy/WO_3

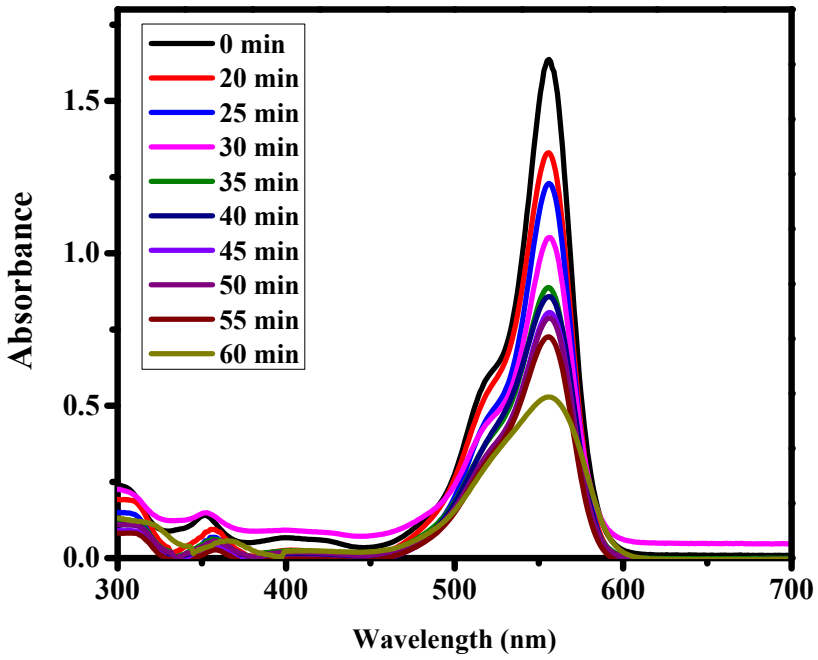

Fig. S9 UV-visible spectra of the degraded samples of Rhodamine B against PPy/WO_3/MWCNT

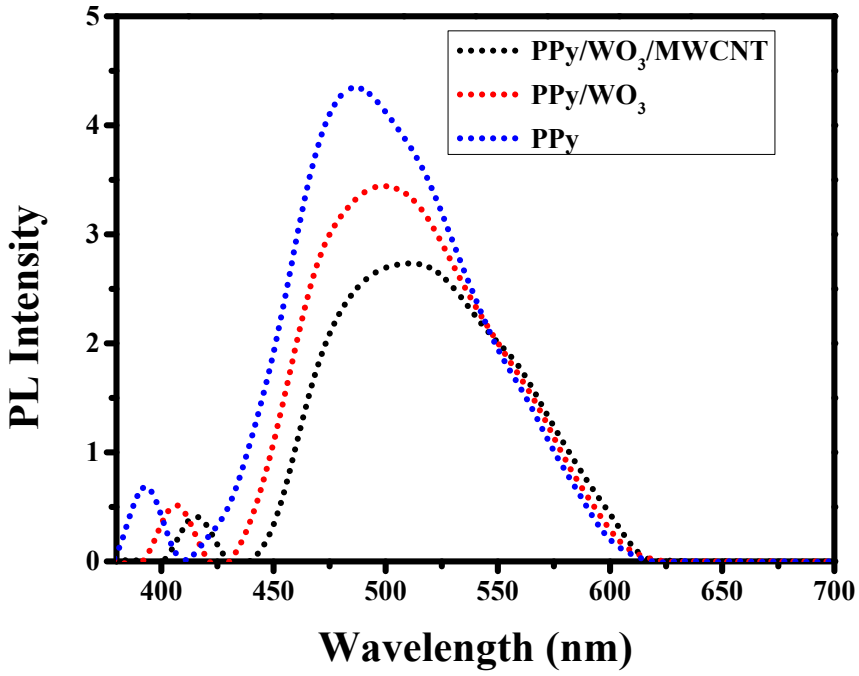

Fig. S10. PL spectra of PPy, PPy/WO_3 and PPy/WO_3/MWCNT

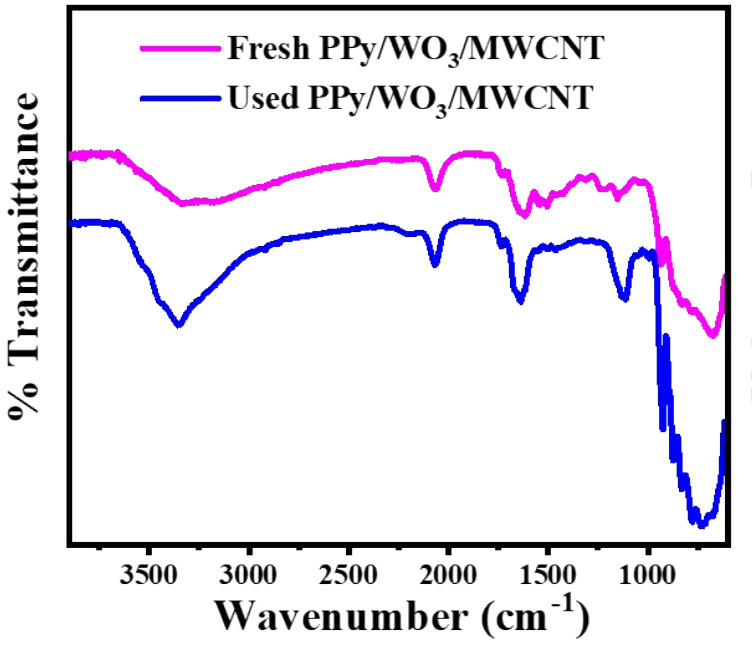

Fig. S11. FTIR spectra of PPy/WO_3/MWCNT catalyst before and after cyclic stability of dye degradation

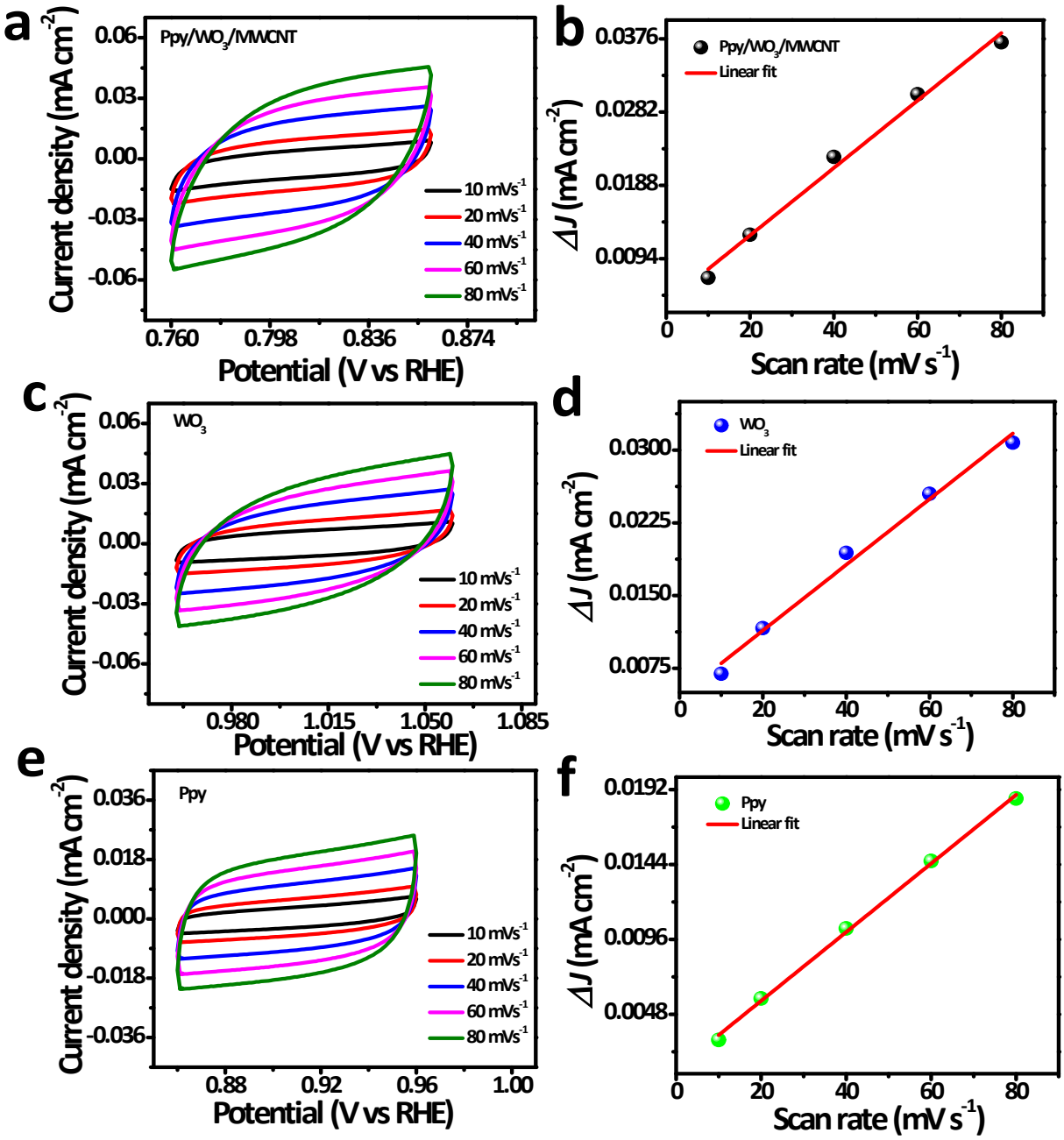

Fig. S12. Electrochemical active surface area analysis (a) CV curves of PPy/WO_3/MWCNT at different scan rate (b) Linear fitting of capacitive currents of the PPy/WO_3/MWCNT electrocatalyst vs scan rate (c) CV curves of WO_3 at different scan rate (d) Linear fitting of capacitive currents of the WO_3 electrocatalyst vs scan rate. (e) CV curves of PPy at different scan rate (f) Linear fitting of capacitive currents of the PPy electrocatalyst vs scan rate.

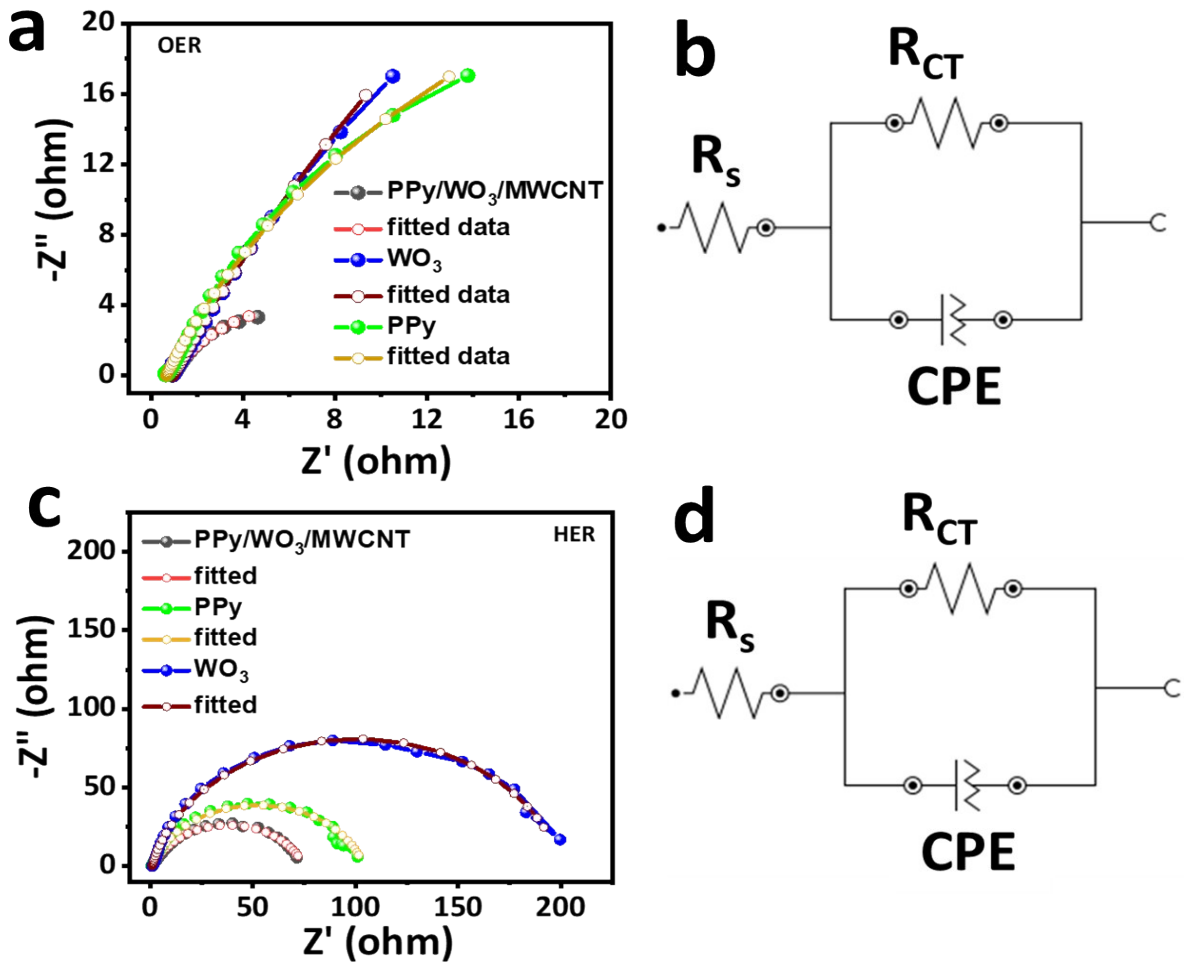

Fig. S13. (a) EIS plot of PPy/WO_3/MWCNT, PPy and WO_3 catalyst materials and corresponding (b) fitted circuit in OER region. (c) EIS plot of PPy/WO_3/MWCNT, PPy and WO_3 catalyst materials and corresponding (d) fitted circuit in HER region in alkaline media.

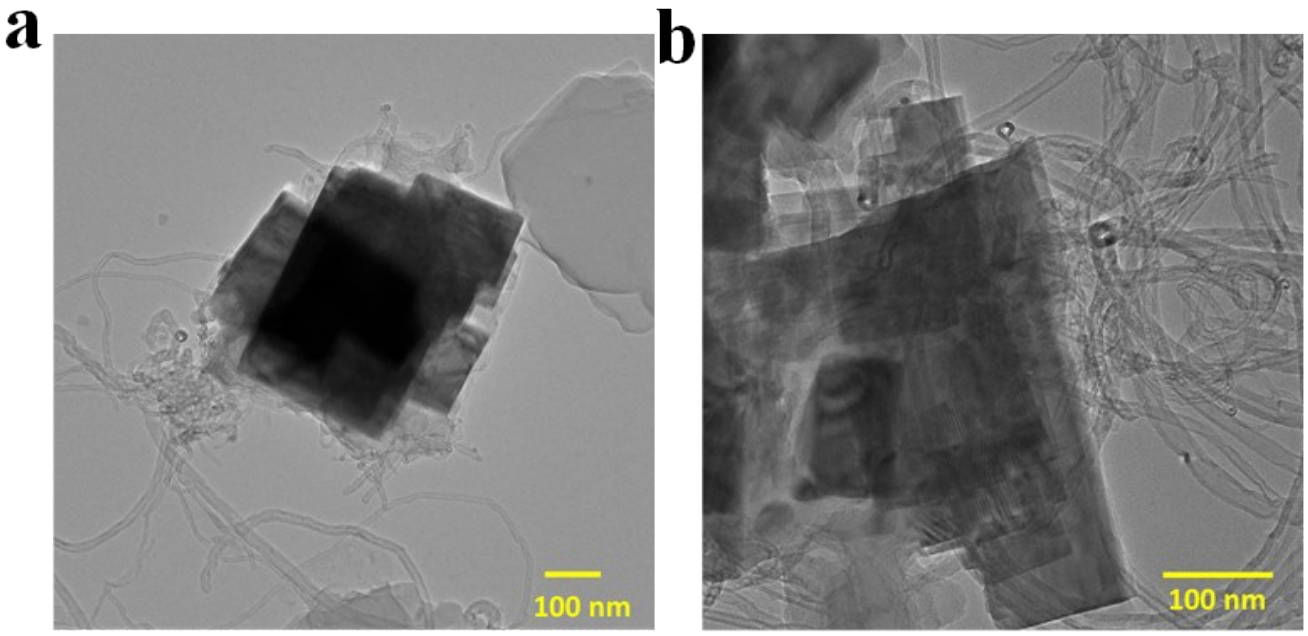

Figure S14. (a-b) TEM Images of the PPy/WO_3/MWCNT catalyst after electrochemical stability analysis.

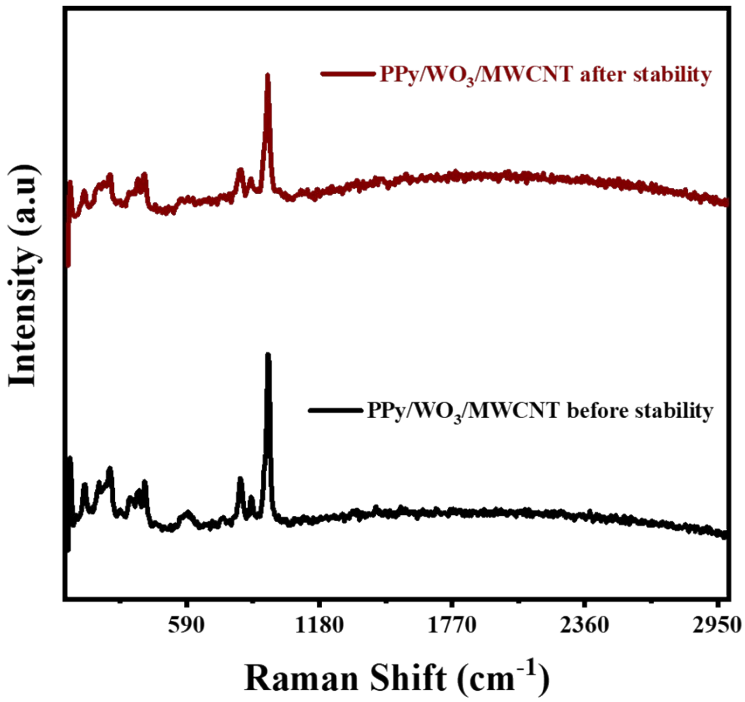

Figure S15. Raman spectra of the PPy/WO_3/MWCNT catalyst before and after electrochemical stability analysis.

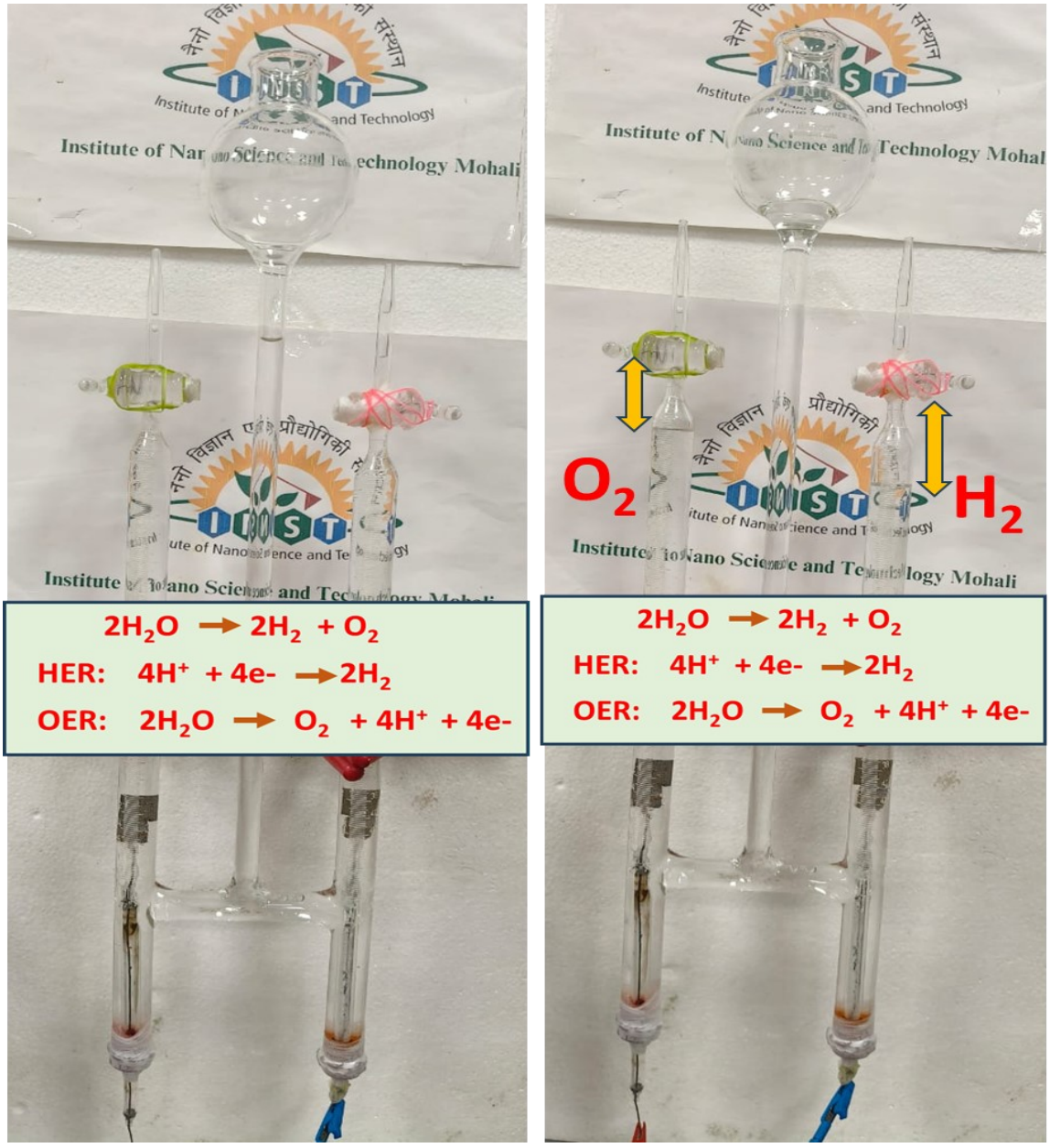

Figure S16. Water-gas displacement setup using electrodes PPy/WO_3/MWCNT (cathode and anode) before and after 60 min emerged in 1.0 M KOH in a Hofmann voltameter using the chronopotentiometry technique.

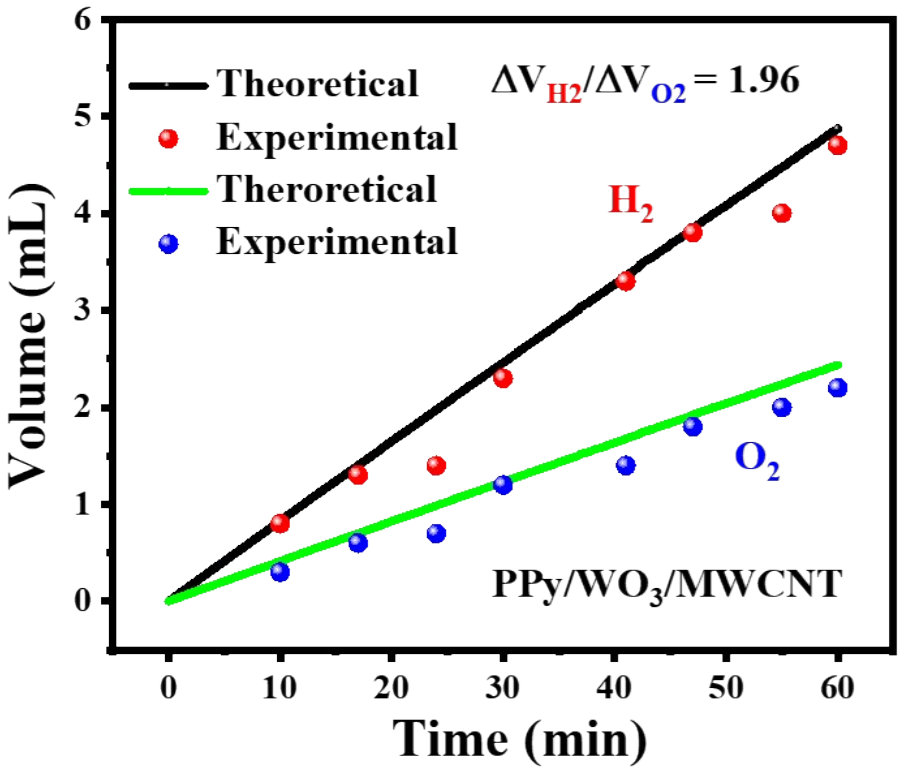

Figure S17. Faradaic efficiency calculation of H_2 and O_2 produced during electrolysis with the PPy/WO_3/MWCNT catalyst.

Table S1: Comparison table for the recently reported catalyst for water splitting

Catalysts	**Overpotential for HER at 10 mA cm^{-2} (mV)**	**Overpotential for OER at 10 mA cm^{-2} (mV)**	**Electrolyte Media**	**Overall water splitting ($E_{j=10}$)**	**Reference**
Cobalt-Phosphorous derived films	94 mV	345 mV	1.0 M KOH	1.56	[1]
Cobalt based Metal Organic Frameworks	154 mV	319 mV	1.0 M KOH	1.55	[2]
$NiCo_2S_4$ nanowires supported on Ni foam	210 mV	260 mV	1.0 M KOH	1.63	[3]
Nickel Phosphide	220 mV	290 mV	1.0 M KOH	1.63	[4]
TiN@Ni_3N Nanowires	21 mV	350 mV	1.0 M KOH	1.64	[5]
Porous MoO_2 Nanosheet	27 mV	260 mV	1.0 M KOH	1.52	[6]
Ru-Ni sandwiched nanoplates	173 mV	270 mV	1.0 M KOH	1.68	[7]
FeCo- N doped carbon nanosheets	150 mV	-----	1.0 M KOH	1.60	[8]
SnO_2/MWCNTs/PANI	524 mV	---	0.5 M KOH	---	[9]
$CoSe_2$/rGO/MWCNT	67 mV		1.0 M KOH		[10]
$NiSe_2$-nanooctahedrons/NF	119 mV	---	1.0 M KOH	1.55 V	[11]
$CoTe_2$–WTe_2 nanostructures	178 mV	184mV	1.0 M KOH	1.52 V	[12]
CoTe/MnO_2/BN	-----	273 mV	1.0 M KOH	--	[13]
MVBG composite	178 mV	273 mV	3.0 M KOH	1.62 V	[14]
rGO/MnO_2/MoS_2	205 mV	208 mV	1.0 M KOH		[15]
Fe_2O_3/MoS_2/$Ti_3C_2T_x$ MXene	123 mV	---	1.0 M KOH	---	[16]
Pt/C + RuO_2	**45 mV**	**325 mV**	**1.0 M**	**1.59 V**	**This study**

			KOH		
PPy/WO_3/MWCNT Nanocomposite	**146 mV**	**328 mV**	**1.0 M KOH**	**1.71**	**This study**

References

1 N. Jiang, B. You, M. Sheng and Y. Sun, *Angew. Chemie - Int. Ed.*, 2015, **54**, 6251–6254.

2 B. You, N. Jiang, M. Sheng, S. Gul, J. Yano and Y. Sun, *Chem. Mater.*, 2015, **27**, 7636–7642.

3 A. Sivanantham, P. Ganesan and S. Shanmugam, *Adv. Funct. Mater.*, 2016, **26**, 4661–4672.

4 L. A. Stern, L. Feng, F. Song and X. Hu, *Energy Environ. Sci.*, 2015, **8**, 2347–2351.

5 Q. Zhang, Y. Wang, Y. Wang, A. M. Al-Enizi, A. A. Elzatahry and G. Zheng, *J. Mater. Chem. A*, 2016, **4**, 5713–5718.

6 Y. Jin, H. Wang, J. Li, X. Yue, Y. Han, P. K. Shen and Y. Cui, *Adv. Mater.*, 2016, **28**, 3785–3790.

7 Y. Zhang, Q. Shao, S. Long and X. Huang, *Nano Energy*, 2018, **45**, 448–455.

8 M. Li, T. Liu, X. Bo, M. Zhou and L. Guo, *J. Mater. Chem. A*, 2017, **5**, 5413–5425.

9 M. Z. Khan, I. H. Gul, M. M. Baig and M. A. Akram, *Electrochim. Acta*, 2023, **441**, 141816.

10 R. Samal, P. Mane, M. Bhat, B. Chakraborty, D. J. Late and C. S. Rout, *ACS Appl. Energy Mater.*, 2021, **4**, 11386–11399.

11 A. K. Nayak and D. Pradhan, *ACS Appl. Energy Mater.*, 2025, **8**, 2088–2102.

12 M. Velpandian, A. Ragunathan, G. Ummethala, S. R. Krishna Malladi and P. Meduri, *ACS Appl. Energy Mater.*, 2023, **6**, 5968–5978.

13 P. Rani, R. Biswas, A. Dutta and P. S. Alegaonkar, *Energy & Fuels*, 2024, **38**, 16809–16819.

14 A. Gowrisankar and S. Thangavelu, *J. Phys. Chem. C*, 2022, **126**, 3419–3431.

15 S. Denisdon, P. Senthil Kumar, C. Boobalan and G. Rangasamy, *Langmuir*, 2024, **40**,

17753–17766.

16 S. DongreS, A. Iqbal, R. Thapa, P. M, S. Ramu and R. G. Balakrishna, *ACS Appl. Eng. Mater.*, 2024, **2**, 943–954.